

# A Parallel-pulling Protocol for Free Energy Evaluation

Van Ngo

*Collaboratory for Advance Computing and Simulations (CACs), Department of Physics and Astronomy,  
University of Southern California, 3651 Watt Way, Los Angeles, California 90089-0242, USA.*

*Email: nvan@usc.edu*

Jarzynski's equality (JE) allows us to compute free energy differences (FEDs) from distributions of work performed on a system. In molecular dynamics simulations, the traditional way of constructing the work distributions is to perform as many simulations as possible. This way does not always produce reliable work distributions in a small number of simulations. The computation cost of that way is not less than other commonly used methods. We show a different way that the distributions of work performed by harmonic potentials can be generated from the distributions of a reaction coordinate (RC) along a pathway. We suggest an alternative method for evaluating FEDs that is based on averaged values of the RC. We propose sequential- and parallel-pulling protocols for generating the work distributions. The requirement for reliable work distributions produced in the protocols is that there must be sufficient mutual overlapping among adjacent configurations along the pathway. The combination of JE and the alternative method can be used to determine the sufficiency of the requirement and the accuracy of computed FEDs. For the stretching of a deca-alanine molecule, our methods require only 19 parallel simulations and relaxation time as small as 0.4 ns for each simulation to estimate FEDs with an uncertainty of about 13%.

## I. INTRODUCTION

In 1997, Jarzynski [1] showed that the free energy change from an initial configuration **A** to a final configuration **B** can be extracted from finite-time non-equilibrium measurements as

$$\Delta F_{\mathbf{A} \rightarrow \mathbf{B}} = -\beta^{-1} \langle \exp(-\beta W) \rangle, \quad (1)$$

where  $\beta = 1/k_{\mathbf{B}}T$ ,  $T$  is temperature,  $k_{\mathbf{B}}$  is Boltzmann constant,  $W$  is applied work and  $\langle \dots \rangle$  denotes the average over all possible trajectories in which work is performed. Those configurations are associated with external control parameters  $\lambda$ . For simplicity, an interested system can be characterized by a single control parameter  $\lambda$  that is used to monitor pathways of a reaction coordinate (RC). If using a harmonic potential (HP) to perform work on the system, parameter  $\lambda$  can be the center of the HP and the center-of-mass position of trapped particles in the direction along  $\lambda$  can be used as an RC. By varying  $\lambda$  from  $\lambda_1$  (corresponding to configuration **A**) at time  $t_1$  to  $\lambda_s$  (corresponding to configuration **B**) at time  $t_s$ , one generates a trajectory or pathway in which applied work  $W$  experimentally measured from a force-versus-extension (FVE) curve is

$$W_{\text{exp}} = \int_{\lambda_1}^{\lambda_s} f_{\lambda} \delta\lambda, \quad (2)$$

where  $f_{\lambda}$  is an applied force measured along the pathway at a value of  $\lambda$  whose increment is  $\delta\lambda$ .

The work definition in Eq. (2) was used to validate Jarzynski's equality (JE) in experiments of slowly stretching a single RNA molecule [2-4]. Since the control parameter  $\lambda$  is varied, the Hamiltonian  $H(\mathbf{z}, \lambda(t))$  of the system accordingly changes with time, where  $\mathbf{z} \equiv (\mathbf{q}, \mathbf{p})$  denotes a point in the phase space with  $\mathbf{q}$  and  $\mathbf{p}$  being coordinates and momenta. According to Jarzynski, work  $W$  can be theoretically evaluated from the Hamiltonian by  $W_{\text{H}} = \int_{t_1}^{t_s} [\partial H(\mathbf{z}, \lambda(t)) / \partial t] dt$  to compute the free energy

change by Eq. (1) [1, 5]. Even if  $W_{\text{H}}$  and  $W_{\text{exp}}$  coincide in slow pulling limits, there is a discrepancy between them. Vilar and Rubi [6] pointed out that using  $W_{\text{H}}$  in Eq. (1) could fail to estimate the free energy change when the Hamiltonian is time-dependent. The definition of work  $W_{\text{H}}$  actually gave rise to a doubt about the validity of JE [7]. By contrast  $f_{\lambda}$ , therefore  $W_{\text{exp}}$ , can be measured without any knowledge of the Hamiltonian. Although Jarzynski identified which work related to Hamiltonian ( $W_{\text{H}}$ ) should be used for JE [8], using mechanical work ( $W_{\text{exp}}$ ) to theoretically investigate the Crooks fluctuation theorem [9-11], which is a more generalized version of JE, has not been widely accepted [12]. In this paper, we will prove that  $W_{\text{exp}}$  should appear in Eq. (1) instead of  $W_{\text{H}}$  to fill the gap between the theory of JE and experiments using JE.

In order to use Eq. (1) for evaluating the free energy change, one has to construct work distributions from all possible FVE curves. In molecular dynamics (MD) simulations, an important question is how to generate correct work distributions in an efficient way [13-18]. Such work distributions should contain rare small values of work since the average of  $\exp(-\beta W)$  is dominated by small values of  $W$ . It is computationally expensive to generate all possible trajectories in MD simulations to sample the work distributions.

One scheme to overcome the computation difficulty is to implement the Potential of Mean Force (PMF) method used by Park *et al.* [13, 18] in Steered Molecular Dynamics (SMD) simulations [19]. In the PMF method  $W$  was defined as  $-vk \int_{t_1}^{t_s} (x - \lambda_1 - vt) dt$ , where  $v$  is a guiding velocity of an HP with spring constant  $k$ . In this definition, parameter  $\lambda$  was assumingly linear with time  $t$ , i.e.,  $\lambda \sim vt$ . In experiments, the definition of work is valid to estimate the free energy change by Eq. (1) if pulling speeds are slow ( $\sim \mu\text{m/s}$ ). In MD simulations, this work is observed to bias free energy changes because MD pulling speeds are many orders of magnitude faster than experimental ones.

The PMF method remedied the biasing problem by utilizing the second order cumulant expansion [13, 18, 20]. Then the computed FEDs were unbiased even with a finite number of trajectories.

Despite of the fact that the PMF method has been increasingly used, the efficiency and accuracy of generating work distributions in complicated systems have remained unsatisfactory. The efficiency is defined as computation cost of evaluating FEDs for a degree of accuracy. Rodriguez-Gomez and Darve [14] showed in the simulations of transfer of fluoromethane across a water-hexane interface that the accuracy of the method based on JE was poor in comparison with their method. Bastug *et al.* [21, 22] showed that it seemed uncertain to obtain unbiased FEDs computed from a finite number of pulling trajectories. The cost of evaluating the FEDs was higher than the cost of using Umbrella Sampling (US) with weighted histogram analysis method [23-25]. Oberhofer *et al.* [15] analyzed that the efficiency of simulations based on JE could not compete with the ones in the US and Thermodynamics Integration [20, 26] methods.

In order to improve the efficiency, one might take the advantage of some attractive features of JE that are parallel, rate-independent and arbitrarily far-from equilibrium. The parallel property means that one can carry out in parallel all pulling trajectories. In contrast, we define a protocol as sequential if a trajectory is generated by sequentially changing  $\lambda$ . Because of the parallel feature, JE promises a faster method for free energy calculations. The method is so-called fast-growth in comparison with the Adaptive Biasing Force (ABF) [14, 27] and US methods. The accuracy of the ABF method is estimated from the analysis of adaptively applied forces on an RC. The accuracy of the US method is improved by allowing multiple overlaps of probability distributions that are associated with the distributions of an RC. These methods suggest a way to improve the accuracy of work distributions that should be related to the quality of the distributions of an RC or of applied forces. We will present a parallel-pulling protocol consisting of the idea for efficiently generating work distributions from the distributions of an RC.

In this article we prove a theory that clarifies the relationship of the work definitions. We take the definition of  $W_H$  as a starting point but treat control parameter  $\lambda$  and time  $t$  in different manners.  $\lambda$  and  $t$  are correlated but not necessarily linear. We prove that mechanical work  $W_{\text{exp}}$  should be the work appearing in Eq. (1) instead of  $W_H$  for the case of canonical ensembles. Our theory suggests another method to compute FEDs from the averaged values of an RC corresponding to different values of  $\lambda$  along a pathway. By discretizing steps of applying an external HP to perform work, we show that it is possible to construct work distributions for Eq. (1) in step-wise pulling simulations. Based on the theory, we propose sequential- and parallel-pulling protocols (SPP and PPP) for implementing the simulations. Based the simulation results, we provide a criterion for ensuring reliable work

distributions produced in SPP and PPP. Our simulation results show that the parallel-pulling protocol speeds up FED calculations with an acceptable accuracy.

Our article is organized as follows: we present our theory in Section II; Section III highlights two methods based on the theory to compute FEDs and describes sequential- and parallel-pulling protocols to implement the methods; the theory is tested in the simulations of unfolding a deca-alanine molecule in Section IV; Section V provides discussions on the theory and methods.

## II. THEORY

Let us consider a system of  $N$  particles described by a time-independent Hamiltonian  $H_o(\vec{p}^{3N}, \vec{r}^{3N})$ , where  $\vec{p}^{3N}$  and  $\vec{r}^{3N}$  are the  $3N$  dimensional momenta and coordinates, respectively. The system has a canonical ensemble with temperature  $T$ . An external harmonic potential (HP)  $U(x, \lambda_i) = k(x - \lambda_i)^2/2$  can be applied to a set of trapped particles, whose center-of-mass position along  $x$ -direction is defined as a reaction coordinate (RC)  $x$ . Here  $\lambda_i$  is the center of the HP (control parameter) and  $k$  is the spring constant. Suppose that there is no coupling between the HP with the particles' momenta. Then our partition functions  $Z(\lambda_i, k)$  ( $i \geq 1$ ) can be simply expressed in terms of spatial coordinates  $(\vec{r}^{3N-1}, x)$  for calculating FEDs.

From time  $t_0$  to  $t_1$ , we apply the HP to the system. One can in principle take the infinity limit for  $t_0$  and  $t_1$ . As a result, the coupling Hamiltonian has the following formula:

$$H(\lambda_1, x) = H_o(\vec{r}^{3N-1}, x) + \frac{k}{2}(x - \lambda_1)^2 \theta(t - t_0) \theta(t_1 - t), \quad (3)$$

where  $\theta(t)$  is a Heaviside step function. Here we have omitted momenta in  $H_o$  for simplicity. Then the work applied to the system from a specific state at  $t = t_0$  to a final state is computed as

$$W_H = \int_{t_0}^{t_1} \frac{\partial H(\lambda_1, x)}{\partial t} dt = \frac{k}{2} \left( (x_0 - \lambda_1)^2 - (x_1 - \lambda_1)^2 \right), \quad (4)$$

where  $x_0$  is an initial value of the RC belonging to the ensemble with  $H_o(\vec{r}^{3N-1}, x_0)$  at time  $t_0$  and  $x_1$  is any final value of the RC at  $t_1 \geq t_0$  belonging to the ensemble with  $H(\lambda_1, x_1)$ . The applied force exerted on the RC along  $x$ -direction at time  $t_1$  is  $f(x_1, \lambda_1) = -\partial U(x_1, \lambda_1)/\partial x_1$ .

If the canonical ensemble of  $x_1$  is generated after turning on the HP, it is possible to take the average of  $\exp(-\beta W_H)$  ( $\beta = 1/k_B T$ ) over the canonical ensemble (see Appendix A) to obtain

$$\left\langle \exp\left[\beta \frac{k}{2} (x_1 - \lambda_1)^2\right] \right\rangle_{(x_1, \lambda_1, k)} = \exp[\beta \Delta F(\lambda_1, k)], \quad (5)$$

where  $(x_1, \lambda_1, k)$  represents all possible points with Hamiltonian  $H(\lambda_1, x_1)$  in phase space and  $\Delta F(\lambda_{i=1}, k) = F(\lambda_{i=1}, k) - F_0 = -\beta \log[Z(\lambda_{i=1}, k)] + \beta \log[Z(0)]$ . The partition functions are  $Z(\lambda_i, k) = \int d\vec{r}^{3N-1} dx_i \exp[-\beta H(\lambda_i, x_i)]$  and  $Z(0) = \int d\vec{r}^{3N-1} dx_0 \exp[-\beta H_o(\vec{r}^{3N-1}, x_0)]$ .  $\Delta F(\lambda_{i=1}, k)$  is the FED between the configurations with and without the HP.

Alternatively, given the canonical ensemble of  $x_0$  the average can be taken over all  $x_0$  instead of  $x_1$  to evaluate the same FED:

$$\Delta F(\lambda_1, k) = -\beta^{-1} \log \left\langle \exp \left[ -\beta \frac{k}{2} (x_0 - \lambda_1)^2 \right] \right\rangle_{(x_0, k=0)}, \quad (6)$$

where  $(x_0, k=0)$  represents all possible points with Hamiltonian  $H_o(\vec{r}^{3N-1}, x_0)$  in phase space. From Eqs. (5) and (6) along with inequality  $\langle \exp(-\beta W_H) \rangle \geq \exp(-\beta \langle W_H \rangle)$  [28], we have the lower and upper bounds to  $\Delta F(\lambda_1, k)$ :

$$\begin{aligned} \left\langle \frac{k}{2} (x_1 - \lambda_1)^2 \right\rangle_{(x_1, \lambda_1, k)} &\leq \Delta F(\lambda_1, k) \\ &\leq \left\langle \frac{k}{2} (x_0 - \lambda_1)^2 \right\rangle_{(x_0, k=0)}. \end{aligned} \quad (7)$$

Now, we perform a series of steps with  $\lambda_i$  ( $i = 1, 2, \dots, s$ ) to pull the RC by moving the center of the HP from  $\lambda_1$  to  $\lambda_s$ . At each step with  $\lambda_i$  the system is relaxed from time  $t_{i-1}$  to  $t_i$ . Then the center of the HP is instantaneously shifted from  $\lambda_i$  to  $\lambda_{i+1}$  at time  $t_i$ . As a result, the total work (see Appendix B) is

$$\begin{aligned} W_{\text{total}} &= \sum_{i=1}^s \frac{k}{2} \left[ (x_{i-1} - \lambda_i)^2 - (x_i - \lambda_i)^2 \right] \\ &= \frac{k}{2} \left[ (x_o - \lambda_1)^2 - (x_s - \lambda_s)^2 \right] + W_{\text{mech}}, \end{aligned} \quad (8)$$

where mechanical work  $W_{\text{mech}}$  in each generated trajectory is defined by

$$W_{\text{mech}} = \frac{k}{2} \sum_{i=1}^{s-1} (\lambda_{i+1} - \lambda_i) (\lambda_{i+1} + \lambda_i - 2x_i) \approx \int_{\lambda_1}^{\lambda_s} f_\lambda \delta\lambda, \quad (9)$$

where  $f_\lambda = \partial U(x, \lambda) / \partial \lambda$  for a sufficiently small increment  $\delta\lambda$ . If  $s$  is equal to 1,  $W_{\text{mech}}$  is zero and Eqs (5) or (6) should be used to estimate FEDs. Equation (8) indicates that in general  $W_{\text{total}}$  (or  $W_H$ ) is different from  $W_{\text{mech}}$ . In infinitely slow pulling limit (large  $s$ ), the first term in Eq. (8) is negligible and  $W_{\text{total}} \cong W_{\text{mech}}$ . Equation (9) can be expressed as  $\sum_{i=1}^{s-1} [H(\lambda_{i+1}, x_i) - H(\lambda_i, x_i)]$  that was used to calculate FEDs in stochastic processes [29].

It should be noted that the canonical ensembles with  $H(\lambda_i, x_i)$  for different  $\lambda_i$  are independent of one another. Hence, it is possible to take average of  $\exp(-\beta W_{\text{total}})$  over all the canonical ensembles of  $x_0, x_1, \dots, x_s$  at the same time to arrive at the following identity:

$$\langle \exp(-\beta W_{\text{total}}) \rangle_{(x_0, x_1, \dots, x_s)} = 1. \quad (10)$$

Alternatively we first average  $\exp(-\beta W_{\text{total}})$  over all  $x_0$ , which correspond to  $H_o(\vec{r}^{3N-1}, x_0)$ , and all  $x_s$ , which correspond to  $H(\lambda_s, x_s) = H_o(\vec{r}^{3N-1}, x_s) + U(x_s, \lambda_s)$ , to obtain

$$\begin{aligned} \langle \exp(-\beta W_{\text{total}}) \rangle_{x_0, x_s} &= \exp \left\{ \beta [F(\lambda_s, k) - F(\lambda_1, k)] \right\} \\ &\quad \times \exp(-\beta W_{\text{mech}}). \end{aligned} \quad (11)$$

We then average the left hand side of Eq. (11) over all the rest of  $x_i$  and make use the equality Eq. (10) to arrive at

$$\langle \exp(-\beta W_{\text{mech}}) \rangle_{\text{FVE}} = \exp[-\beta \Delta F^{\text{JE}}(\lambda_s, \lambda_1, k)], \quad (12)$$

where  $\Delta F^{\text{JE}}(\lambda_s, \lambda_1, k) = F(\lambda_s, k) - F(\lambda_1, k)$  with  $F(\lambda_i, k) = -\beta \log \langle Z(\lambda_i, k) \rangle$  and  $\langle \dots \rangle_{\text{FVE}}$  is the average over all values of  $W_{\text{mech}}$  measured from force-versus-extension (FVE) curves (detailed derivation of Eq. (12) is given in Appendix B). Equation (12) is identical to JE Eq. (1). The definition of mechanical work  $W_{\text{mech}}$  defined by Eqs. (2) or (9) does give us the desired FED  $\Delta F^{\text{JE}}(\lambda_s, \lambda_1, k)$ .

It is noted that the distributions of  $x_i$  have the property of randomness due to thermal fluctuations. According to the probability theory of independent random numbers [30],  $W_{\text{mech}}$ 's distribution  $\rho(W_{\text{mech}})$  is proportional to  $\rho(x_1)\rho(x_2)\dots\rho(x_{s-1})$  where  $\rho(x_i)$  are  $x_i$ 's distributions. The relation between  $\rho(W_{\text{mech}})$  and  $\rho(x_i)$  means that  $\rho(W_{\text{mech}})$  can be constructed if a set of  $\rho(x_i)$  is known.

Since the RC is trapped by the HP,  $\rho(x_i)$  can be approximated as  $\exp[-\beta k(x_i - \langle x_i \rangle)^2 / (2\gamma_i^2)]$ , where  $\langle x_i \rangle$  is the averaged position of the RC at  $i^{\text{th}}$  pulling step and  $\gamma_i^2$  is  $k\sigma_i^2/k_B T$  with  $\sigma_i$  equal to the standard deviation of  $x_i$ 's distribution. Thus  $\rho(W_{\text{mech}})$  can be expressed in terms of  $x_i$ ,  $\langle x_i \rangle$  and  $\gamma_i^2$  with  $i$  from 1 to  $s-1$ . Given the distribution of  $W_{\text{mech}}$  and based on Eq. (12) we derive a simple relationship between Gaussian-approximated FED  $\Delta F^{\text{G}}(\lambda_s, \lambda_1, k)$  and  $\langle x_i \rangle$  (see Appendix B):

$$\begin{aligned} \Delta F^{\text{G}}(\lambda_s, \lambda_1, k) &= \frac{k(\lambda_s - \lambda_1)^2}{2s} \frac{\sum_{i=1}^{s-1} (1 - \gamma_i^2)}{s} \\ &\quad + k(\lambda_s - \lambda_1) \frac{\sum_{i=1}^{s-1} (\lambda_i - \langle x_i \rangle)}{s}. \end{aligned} \quad (13)$$

The first term in Eq. (13) vanishes as  $s$  goes to infinity, i.e., infinitely slow pulling limit. Then the FED  $\Delta F^{\text{G}}(\lambda_s, \lambda_1, k)$  can be determined from the second term,

$$\Delta F_{\text{fluct}}(\lambda_s, \lambda_1, k) = k(\lambda_s - \lambda_1) \frac{\sum_{i=1}^{s-1} (\lambda_i - \langle x_i \rangle)}{s}, \quad (14)$$

which only depends on the average of the differences between  $\lambda_i$  and  $\langle x_i \rangle$ . In that limit, the left hand side of Eq. (14) becomes the Thermodynamics Integration (TI)  $\int_{\lambda_1}^{\lambda_s} \langle \partial H(\lambda, x) / \partial \lambda \rangle_\lambda d\lambda$ . This limit implies that the required relaxation time  $\tau_i = t_i - t_{i-1}$  at each  $\lambda_i$  can be arbitrarily small. Moreover, if all  $\gamma_i^2$  are unity,  $\Delta F^{\text{G}}(\lambda_s, \lambda_1, k)$  can also be determined from  $\Delta F_{\text{fluct}}(\lambda_s, \lambda_1, k)$  even with a finite value of  $s$ .  $\gamma_i^2$  equal to unity indicates that  $x_i$ 's distributions resemble the canonical distributions of the system ( $\sim \exp[-\beta U(x_i, \lambda_i)]$ ). The condition for  $\gamma_i^2$  equal to unity is satisfied if  $\tau_i$  is large (the assumption for canonical distributions). These two limiting cases of  $\tau_i$  suggest that the first term in Eq. (13) is not important and Eq. (14) can be used to evaluate FEDs with finite  $s$  and finite  $\tau_i$ .

We find that there is an extra requirement for using Eqs. (12) and (14) that will be pointed out in the following section.

### III. Protocol

Based on our theory in the previous section, we propose two methods for free energy calculations: (i) from the distributions of mechanical work  $W_{\text{mech}}$  that is defined by Eq. (9) using JE, i.e., Eq. (12); (ii) from averaged values of  $\langle x_i \rangle$  using Eq. (14). There are two protocols described in the followings to implement the methods.

According to JE Eq. (12), it is necessary to generate as many pulling trajectories ( $N_p$ ) as possible in parallel to construct work distributions (see Fig. 1a). The configuration **A** in the original protocol requires a Gaussian distribution of states sampled from an arbitrarily initial state  $x_o$  in which there is no applied potential. We find that this protocol is not the unique way to construct work distributions. The expression of  $W_{\text{mech}}$  (Eq. 9) in terms of  $x_i$  suggests that work distributions can be constructed from the distributions of  $x_i$ . Importantly, this expression implies that rare small values of work cannot be produced if the increments  $\lambda_{i+1}-\lambda_i$  are larger than the magnitudes of  $x_i$ 's fluctuations. This implication enforces a specific requirement for generating  $x_i$ 's distributions that must have some mutual overlapping among them.

We now propose two protocols, as illustrated in Fig. 1b, to construct work distributions and compute FEDs based on Eqs. (12) and (14):

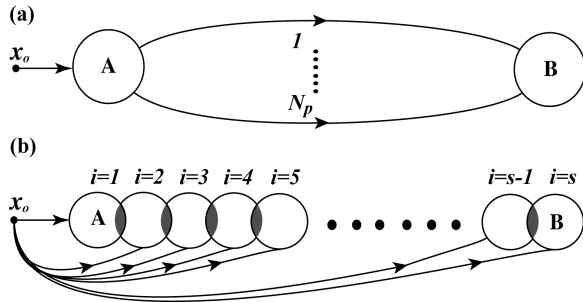


FIG. 1. Schematic illustration for (a) original parallel pulling (arrowed arcs) protocol (b) our proposed sequential (series of circles) and parallel pulling (arrowed arcs) protocols. An RC,  $x_o$ , represents any state without virtual harmonic potentials. The arcs with arrows represent parallel pulling trajectories. **A** and **B** are initial and final configurations, respectively.  $N_p$  is a number of trajectories. The circles represent sets of states or distributions of the RC. Shaded areas are mutual overlapping states. Index  $i$  denotes the ordered number of pulling and runs from 1 to  $s$ , where indices 1 and  $s$  also represent the initial and final configurations, respectively.

(i) Sequential step-wise pulling protocol (SPP): given a pathway that can be characterized by a single control parameter  $\lambda$  (the center of an HP), we assign  $\lambda_1$  to the configuration **A**,  $\lambda_s$  to the configuration **B**. We then divide the pathway into  $s-2$  intermediate configurations (steps) that are characterized by different  $\lambda_i$ . We let the HP pull the RC in a single simulation by sequentially assigning  $\lambda$  to be  $\lambda_i$  with  $i$  from 1 to  $s$ . At each step corresponding to  $\lambda_i$ , the system is relaxed with relaxation time  $\tau_i$  so that there is mutual overlapping among successive distributions

of  $x_i$ . All possible values of  $x_i$  along the pathway are collected to generate work distributions (see Appendix C).

(ii) Parallel pulling protocol (PPP): given a pathway and a set of different  $\lambda_i$  corresponding to  $s$  targeted configurations like the protocol (i),  $s$  pulling simulations are independently carried out to pull the RC from a state  $x_o$  to the targeted configurations. In each simulation, the center of an HP  $\lambda$  is independently assigned to be  $\lambda_i$  with  $i$  from 1 to  $s$ . Each simulation requires adequate relaxation time  $\tau_i$  so that there is mutual overlapping among distributions of  $x_i$  corresponding to  $\lambda_i$ . The way to construct work distributions in this protocol is the same as in the protocol (i).

When work distributions are constructed, it is straightforward to evaluate FEDs based on JE Eq. (12). By measuring all averaged values of  $x_i$  corresponding to  $\lambda_i$ , we compute FEDs based on Eq. (14) in either the sequential or parallel pulling protocols.

The protocols are reasonable. Equation (5) supports that a FED  $\Delta F(\lambda_i, k)$  can be calculated if a complete canonical ensemble of  $x_i$  is sampled regardless of pathways from  $x_o$ . But merely using Eq. (5) to compute the FED is expensive. In many cases it is elusive to know when the ensemble is canonical [31]. In other words, the canonical ensemble requires large  $\tau_i$  to be generated. The implementation of the protocols in Section IV will show that  $\tau_i$  in our protocols can be much smaller. The combination of un-fully canonical distributions of  $x_i$  having mutual overlapping turns out to be sufficient to evaluate FEDs. In the following Section, the requirement of the mutual overlapping will be discussed in the tests of the protocols against the accuracy of computed FEDs.

## IV. IMPLEMENTATION AND TESTING

In this section we use the two protocols to apply the two methods to an exemplary system: helix-coil transition of deca-alanine in vacuum at  $T = 300$  K (see Ref. [13] for more details of simulation setups). NAMD2 package [32] and CHARMM22 force fields [33] are used here. We generate work distributions and compute free energy profiles by both the methods in sequential (a) and parallel (b) pulling protocols. We investigate the effects of spring constants  $k$  (c) and relaxation time  $\tau_i = \tau$  for all pulling steps (d).

### A. Sequential pulling protocol (SPP)

The simulation setups are kept the same as studied by Park *et al.* [13]. One end of the molecule is kept fixed at the origin. The other end is sequentially pulled by a harmonic potential (HP) having the spring constant  $k = 7.2$  kcal/mol/Å<sup>2</sup> (we use this HP through the paper otherwise clearly mentioned). The position along the pulling direction of the pulled end is considered as a reaction coordinate (RC). Instead of continuously varying the center of the HP  $\lambda$  (control parameter) with time (i.e. every time-step), we increase  $\lambda$  by  $\Delta\lambda = 0.5$  Å from  $\lambda_1 = 13$  to  $\lambda_s$

= 31 Å ( $s = 39$ ). At each step with  $\lambda_i$  ( $i = 1, 2, \dots, s$ ) the system is relaxed for  $\tau = 10$  ns. Hence, the averaged pulling speed is 5.0 nm/s. Every 0.1 ps at each relaxation step (RS) we record the position of the pulled end  $x_i$ . This data set of  $x_i$  is used to construct the distributions as briefly shown in Fig. 2a. We use Least Square Fitting method to obtain  $\gamma_i^2$  as shown by the inset in Fig. 2b. The dimensionless values of  $\gamma_i^2$  fall in the range of 1.1 to 1.4 and are peaked at  $\lambda = 25$  Å. The highest value of  $\gamma_i^2$  occurs at the same position where the free energy profiles are observed to be a plateau (see Fig. 3a). This position can be considered as a barrier position or a transition point. The values of  $\gamma_i^2$  indicate how the approximated widths of  $x_i$ 's distributions relatively change along our pathway.

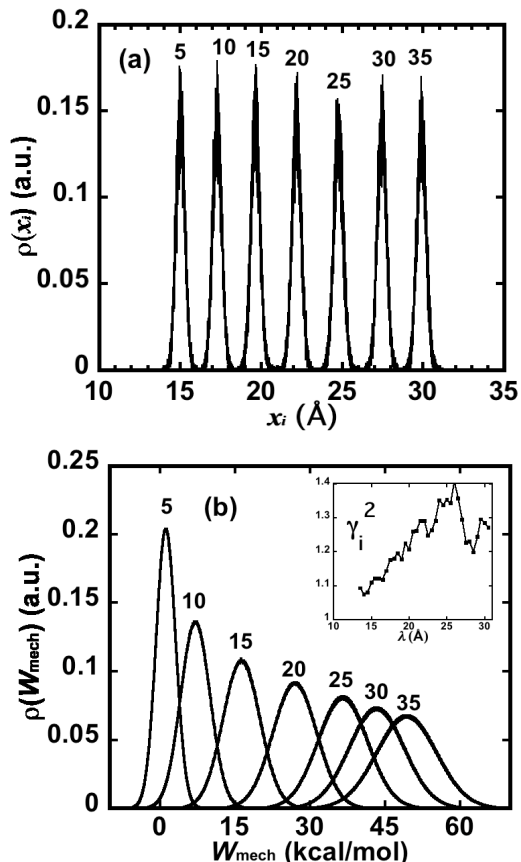


FIG. 2. Distributions of  $x_i$  (a) and of mechanical work  $W_{\text{mech}}$  (b) from steps  $i = 5$  ( $\lambda = 15$  Å) to  $i = 35$  ( $\lambda = 30$  Å). The inset shows  $\gamma_i^2$  versus  $\lambda$ .

We divide the ranges of  $x_i$  and  $W_{\text{mech}}$  into small bins to generate work distributions (see Appendix C) as briefly shown in Fig. 2b. The work distributions change as  $\lambda$  increases. Plugging these distributions and measured  $\langle x_i \rangle$  into Eqs. (9), (12), (13) and (14), we compute applied mechanical work  $W_{\text{mech}}$ , FEDs  $\Delta F^{\text{JE}}$ ,  $\Delta F^{\text{G}}$  and  $\Delta F_{\text{fluct}}$  as functions of  $\lambda$ , respectively. The referenced free energy for those FEDs is  $F(\lambda_1, k)$  that is used through out the paper whenever we discuss the FEDs.  $\lambda$  and  $k$  are omitted in the functions for a simple notation. The PMF profile is

generated by the PMF method with the pulling speed of  $v=0.1$  Å/ns for comparison.

Figure 3a shows that the profiles of  $\Delta F^{\text{JE}}$  and  $\Delta F_{\text{fluct}}$  are in a good agreement with the PMF profile. At the minimum position ( $\lambda \sim 15$  Å)  $\Delta F^{\text{JE}}$  is the same as that of the PMF profile ( $\sim -2.1$  kcal/mol) that is lower than  $\Delta F_{\text{fluct}}$  by 0.5 kcal/mol. At  $\lambda \geq 25$  Å (barrier position), the values of the PMF profile are larger than  $\Delta F_{\text{fluct}}$  by 1.0 kcal/mol, but only differ from  $\Delta F^{\text{JE}}$  ( $\geq 16$  kcal/mol) by 0.5 kcal/mol. Free energies  $\Delta F^{\text{G}}$  are lower than the others because the effects of finite  $s$  and  $\tau$  cause a significant contribution to  $\Delta F^{\text{G}}$ . The lower values of  $\Delta F^{\text{G}}$  and the agreement between the profile of  $\Delta F_{\text{fluct}}$  and the PMF profile confirm the argument at the end of Section II that the first term in Eq. (13) is not important for evaluating FEDs.

## B. Parallel pulling protocol (PPP)

The agreement between  $\Delta F_{\text{fluct}}$  [Eq. (14)] and  $\Delta F^{\text{JE}}$  [Eq. (12)] suggests that one can compute FEDs if the values of  $\langle x_i \rangle$  and their fluctuations are known in any pulling protocols. To verify this observation, we perform 19 10ns-simulations in parallel of stretching the molecule from the same initial state  $x_0$  to final states. In the simulations 19 values of  $\lambda_i$  are assigned to be 13, 14...31 Å ( $\Delta\lambda = 1$  Å and  $s = 19$ ). In this PPP each simulation characterized by a single value of  $\lambda_i$  is independent of the others. At each step with  $\lambda_i$  we record all values of  $x_i$  in every 0.1 ps for constructing work distributions. For comparison with the previous pulling simulations in Part A, we keep the relaxation time the same ( $\tau = 10$  ns).

The computed profile of  $\Delta F_{\text{fluct}}$  is plotted in Fig. 3b together with the one obtained in Part A. Figure 3b shows that  $\Delta F_{\text{fluct}}$  in both the SPP and PPP have the same minimum FED. For larger values of  $\lambda$ , the profile of  $\Delta F_{\text{fluct}}$  in the PPP is gradually shifted below the one in the SPP by an amount of 1.0 kcal/mol. With these data of  $x_i$  we generate work distributions and evaluate  $\Delta F^{\text{JE}}$  as shown in Fig. 3b. The minimum value of  $\Delta F^{\text{JE}}$  is slightly lower than those of  $\Delta F_{\text{fluct}}$ . The values of  $\Delta F^{\text{JE}}$  in the PPP are only 2.0 kcal/mol larger than those of  $\Delta F_{\text{fluct}}$  in the SPP at  $\lambda \geq 25$  Å.

We observe that the separation between the profiles of  $\Delta F^{\text{JE}}$  and  $\Delta F_{\text{fluct}}$  becomes smaller as  $\Delta\lambda$  is changed from 1.0 Å (see Fig. 3b) to 0.5 Å (see Fig. 3a). The profile of  $\Delta F_{\text{fluct}}$  in the SPP lies between the profiles of  $\Delta F^{\text{JE}}$  and  $\Delta F_{\text{fluct}}$  in the PPP. This suggests that both the  $\Delta F^{\text{JE}}$  and  $\Delta F_{\text{fluct}}$  in the PPP can be combined to estimate the ‘exact’ free energy profile of our system. The free energies of the ‘exact’ profile can be defined as  $(\Delta F^{\text{JE}} + \Delta F_{\text{fluct}})/2$ . Subsequently, the uncertainty of these free energies would be equal to  $(\Delta F^{\text{JE}} - \Delta F_{\text{fluct}})/2$  that is at most 1.5 kcal/mol ( $\sim 10\%$ ) as  $\Delta\lambda = 1.0$  Å. In terms of computation cost, the PPP is definitely at least 20 times faster than the SPP.

It is worth to compare the averaged applied forces in both the SPP and PPP along our pathway. The factor  $k \sum_{i=1}^{s-1} (\lambda_i - \langle x_i \rangle) / s$  in Eq. (14) can be interpreted as

averaged accumulating forces along our pathway. The inset in Fig. 3 shows that the accumulating forces in both the pulling protocols are almost the same. Both of them are saturated after  $\lambda$  equal to 25 Å.

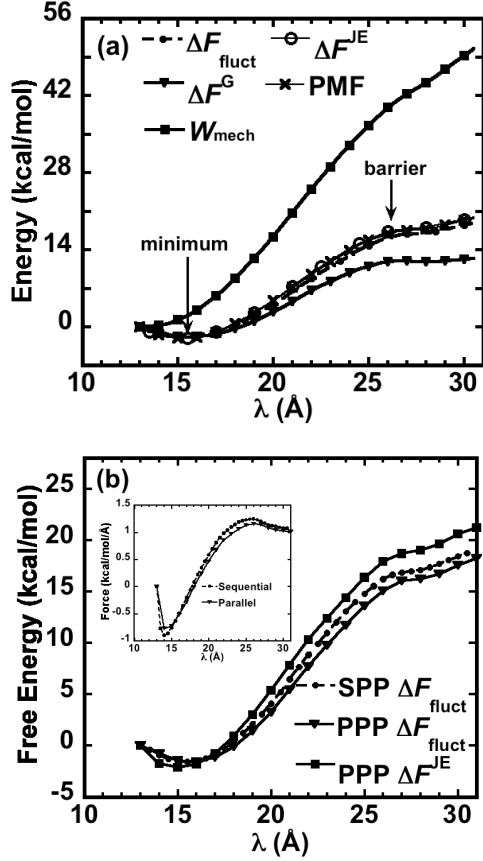


FIG. 3. (a) Mechanical work (boxes), free energies versus  $\lambda$ . PMF (crosses),  $\Delta F^{\text{JE}}$  (empty circles),  $\Delta F^{\text{G}}$  (triangles) and  $\Delta F_{\text{fluct}}$  (dots) are free energies computed by the PMF method, Eq. (12), Eq. (13) and Eq. (14) in the sequential pulling, respectively. (b) Free energies versus  $\lambda$ .  $\Delta F_{\text{fluct}}$  (dots) are in the SPP with  $\Delta\lambda = 0.5$  Å.  $\Delta F_{\text{fluct}}$  (triangles) and  $\Delta F^{\text{JE}}$  (boxes) are in the PPP with  $\Delta\lambda = 1$  Å. The inset shows the accumulating forces  $\Delta F_{\text{fluct}}/(\lambda_s - \lambda_1) = k \sum_{i=1}^{s-1} (\lambda_i - \langle x_i \rangle) / s$  versus  $\lambda$  for both the protocols.

It is possible to collect 10  $x_i$ 's distributions with  $\Delta\lambda = 2$  Å ( $s = 10$ ,  $\lambda_i = 13, 15, \dots, 31$  Å) out of the 19 distributions to construct corresponding work distributions. As a result, the FEDs at  $\lambda = 25$  Å computed from this data set using JE and Eq. (14) are about 31.8 and 11.4 kcal/mol, respectively. In other words, with these data we overestimate the FED if using JE and underestimate it if using Eq. (14). These FEDs clearly indicate that the data set with  $\Delta\lambda = 2$  Å cannot be used to construct correct work distributions and measure a sufficient history of  $\langle x_i \rangle$ . This observation is consistent with the implication of  $W_{\text{mech}}$ 's expression that the increments  $\Delta\lambda = \lambda_i - \lambda_{i-1}$  should not exceed the magnitudes of  $x_i$ 's fluctuations; otherwise rare small values of  $W_{\text{mech}}$  are not available. Figure 2a shows that the magnitudes of  $x_i$ 's fluctuations are about 1.0 Å.

Consequently  $\Delta\lambda$  should be chosen to be not larger than 1.0 Å. It means that  $s$  can be finite but not arbitrarily small.

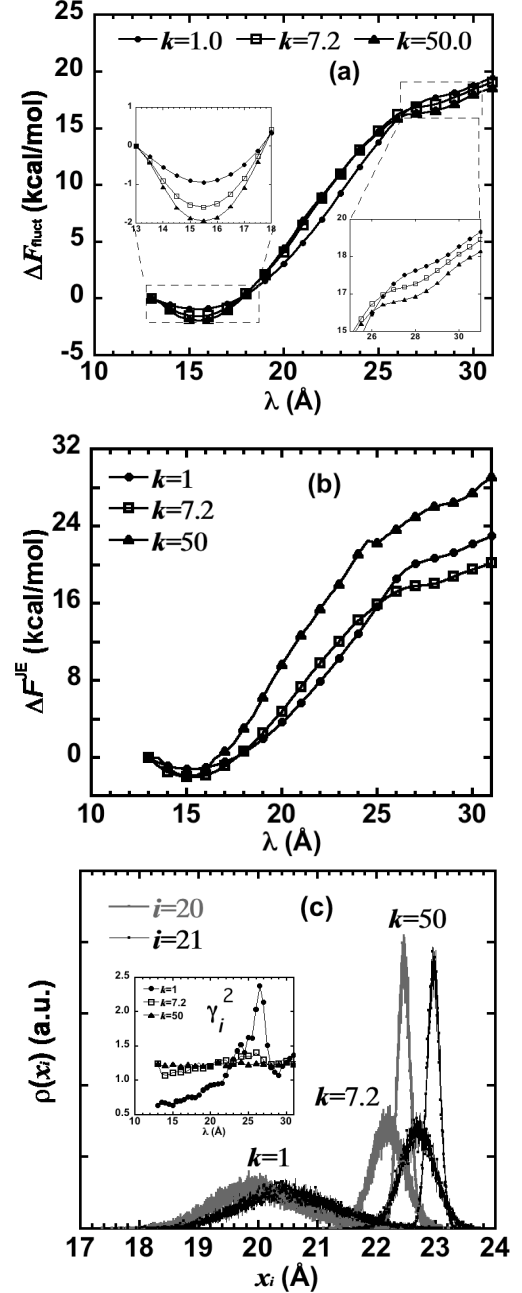


FIG. 4. Free energy profiles of (a)  $\Delta F_{\text{fluct}}$  and (b)  $\Delta F^{\text{JE}}$  with different spring constants  $k=1.0$  (dots), 7.2 (empty boxes) and 50.0 (triangles) kcal/mol/Å<sup>2</sup>. (c) Distributions of  $x_i$  at step  $i = 20$  (gray) and 21 (black) in the three cases. The insets in (a) are zoomed at the minimum and barrier positions. The inset in (c) shows  $\gamma^2$  versus  $\lambda$ .

One can reduce spring constant  $k$  to enlarge  $x_i$ 's fluctuations, however that would require longer relaxation time. Hence, we investigate the effects of spring constants  $k$  and relaxation time  $\tau$  on FEDs in Parts C and D.

### C. Effects of spring constant $k$

In order to investigate how FEDs vary in response to different spring constants  $k$ , we perform two sequential pulling simulations in which  $k = 1.0$  and  $50.0$  kcal/mol/Å<sup>2</sup>,  $\Delta\lambda = 0.5$  Å and  $\tau = 10$  ns are used. It is more convenient to do analysis in these simulations using the SPP than in simulations using the PPP. If the PPP is used, in the case of  $k = 1.0$  kcal/mol/Å<sup>2</sup> one might have to use larger relaxation time  $\tau$  to have good statistics of  $x_i$  at large  $\lambda$  than  $\tau$  at smaller  $\lambda$ .

We observe that the sets of  $\langle x_i \rangle$  in all three cases are not the same. In the case of  $k = 1.0$  kcal/mol/Å<sup>2</sup>  $\langle x_i \rangle$  are not as perfectly linear with  $\lambda$  as in the other cases. But the free energy profiles of  $\Delta F_{\text{fluct}}$  as plotted in Fig. 4a are in a good agreement with one another. The minimum FEDs are  $-0.9$ ,  $-1.6$  and  $-1.9$  kcal/mol corresponding to  $k = 1.0$ ,  $7.2$  and  $50.0$  kcal/mol/Å<sup>2</sup>, respectively. At  $\lambda \geq 25$  Å, the three curves are merging and shifted by  $1.0$  kcal/mol from each other with the same order as appearing at the minimum position (see the insets in Fig. 4a). The smallest spring constant gives us the higher values of the FEDs at the minimum and barrier positions ( $\lambda \sim 15$  and  $26$  Å), while the strongest one gives rise to the smaller values. With the uncertainty of  $2.0$  kcal/mol, we confirm that those important values evaluated by Eq. (14) are independent of spring constants in the range from  $1.0$  to  $50.0$  kcal/mol/Å<sup>2</sup>, even if there is noticeable lowering of the FEDs at  $k = 1.0$  kcal/mol/Å<sup>2</sup> along the pathway from the minimum to the barrier positions.

However, as computed by JE, the free energy profiles are distinguishable as seen in Fig. 4b. The FEDs at both the smaller and larger values of  $k$  are clearly higher than that in the case of  $k = 7.2$  kcal/mol/Å<sup>2</sup> as  $\lambda > 25$  Å. To explain the significant distinction among the profiles, we look at the distributions of  $x_i$  at step  $i = 20$  and  $21$  ( $\lambda \sim 23$  Å) where the transition is about to occur. Figure 4c shows that the two  $x_i$ 's distributions at  $k = 1.0$  kcal/mol/Å<sup>2</sup> are lagging behind the others, whereas at  $k = 50$  kcal/mol/Å<sup>2</sup> they have much less mutual overlapping than the others.  $\gamma_i^2$  in the inset of Fig. 4c indicate how  $x_i$ 's distributions relatively change along our pathway. The smaller values of  $\gamma_i^2$  indicate narrower widths of  $x_i$ 's distributions. Hence they imply less mutual overlapping among the successive distributions since the same increment  $\Delta\lambda = 0.5$  Å is used. In the case of  $k = 1.0$  kcal/mol/Å<sup>2</sup>,  $\gamma_i^2$  having the highest value and the lagging of  $x_i$ 's distributions indicate that  $x_i$  is likely being trapped by the system's local free energy minimum in some previous pulling steps ( $i = 20$  and  $21$ ) before the transition occurs. These observations suggest a possible explanation for the distinction based on the expression of  $W_{\text{mech}}$  in Eq. (9). On one hand with small spring constants, it is possible that the difference between  $\lambda_i$  and  $x_i$  needs to be large for increasing applied forces to pull the RC out of the local minimum. This difference increases the magnitude of work, hence that of computed FEDs. On the other hand with large spring constants, the

OT confines the RC in such narrow regions that the RC's distributions have less mutual overlapping. Consequently, large  $k$  likely reduces number of small values of rare work, thus increases the magnitude of computed FEDs.

### D. Effects of relaxation time $\tau$

We repeat the PPP in Part B by reducing relaxation time  $\tau$  from  $10$  ns to  $0.01$  ns to optimize required time to perform such simulations, particularly for our test case. Spring constant  $k = 7.2$  kcal/mol/Å<sup>2</sup> and increment  $\Delta\lambda = 1.0$  Å ( $s = 19$ ) are used in the simulations for all values of  $\tau$ . We evaluate FEDs  $\Delta F_{\text{fluct}}$  and  $\Delta F^{\text{JE}}$  at  $\lambda = 26$  Å (barrier position). Here we consider those FEDs as functions of  $\tau$ .

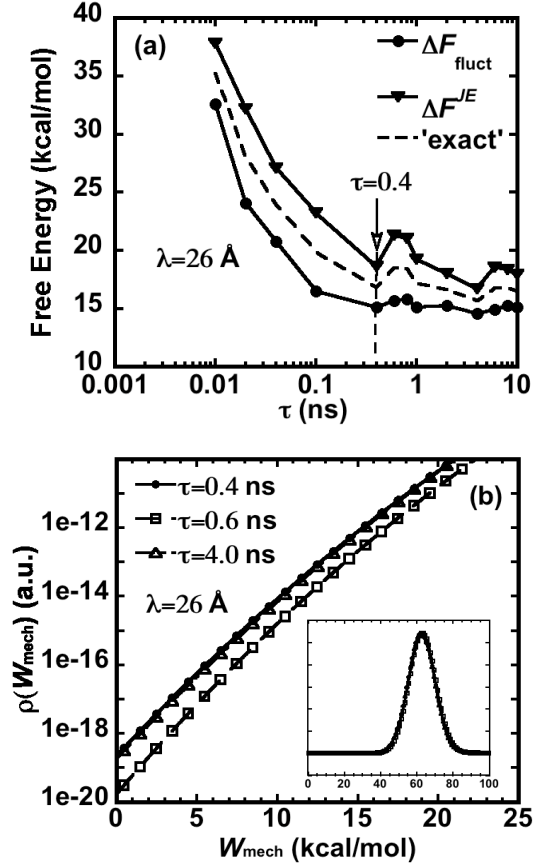


FIG. 5. (a) Free energies  $\Delta F_{\text{fluct}}$  (dots),  $\Delta F^{\text{JE}}$  (full triangles) and  $(\Delta F_{\text{fluct}} + \Delta F^{\text{JE}})/2$ , called 'exact' (dashed line), at  $\lambda = 26$  Å versus relaxation time  $\tau$ . (b) Rare work distributions at  $\lambda = 26$  Å in a range from 0 to 25 kcal/mol at  $\tau = 0.4$  (dots),  $0.6$  (empty boxes) and  $4.0$  (empty triangles) ns. The inset in (b) shows the overall work distributions at the three values of  $\tau$ .

Figure 5a shows how our FEDs change in response to variation of  $\tau$ . The curve of  $\Delta F^{\text{JE}}$  is noticeably higher than the curve of  $\Delta F_{\text{fluct}}$  that starts converging at  $\tau = 0.4$  ns. The convergence of  $\Delta F_{\text{fluct}}$  is due to the strong applied HP that makes the corresponding sets of  $\langle x_i \rangle$  not essentially change even at  $\tau = 0.4$  ns. But  $\Delta F^{\text{JE}}$  does not converge as smoothly as  $\Delta F_{\text{fluct}}$  does. The values of  $\Delta F^{\text{JE}}$  have small peaks at  $\tau = 0.6$  and  $6.0$  ns. These peaks indicate some important

changes in the work distributions. For example as seen in Fig. 5b, the rare work distribution at  $\tau = 0.6$  ns is lower than those at  $\tau = 0.4$  and 4.0 ns. Nevertheless, the inset of Fig. 5b shows no visible deviation among their overall distributions. These rare work distributions have major contributions to  $\Delta F^{\text{JE}}$ . The work having lower distributions gives rise to larger  $\Delta F^{\text{JE}}$ .

In addition, Fig. 5a shows that the separation between  $\Delta F^{\text{JE}}$  and  $\Delta F_{\text{fluct}}$  becomes smaller as  $\tau$  increases. This trend is similar to the trend occurring as we changed  $\Delta\lambda$  from 1.0 Å to 0.5 Å (see Fig. 3). It suggests that the ‘exact’ value of the FED at  $\lambda = 26$  Å as a function of  $\tau$  would be somewhere between the  $\Delta F^{\text{JE}}$  and  $\Delta F_{\text{fluct}}$  as shown by the dashed line in Fig. 5a. The estimate of the ‘exact’ FED is defined as  $(\Delta F^{\text{JE}} + \Delta F_{\text{fluct}})/2$ . The smallest relaxation time can be chosen as small as 0.4 ns. Therefore, the ‘exact’ FED has the uncertainty equal to  $(\Delta F^{\text{JE}} - \Delta F_{\text{fluct}})/2$  or  $\sim 13\%$  at  $\tau = 0.4$  ns.

## V. DISCUSSION AND CONCLUSION

Our theory illustrates a consideration that the correlation between control parameter  $\lambda$  and time  $t$  should be treated carefully. We suggest that  $\lambda$  should not be considered as a linear function of time  $t$ . Parameter  $\lambda$  should be a time-independent parameter characterizing perturbed states. Finite relaxation time  $\tau$  is required to let a system evolve into those perturbed states. The introduction of the double Heaviside function of time  $t$  does describe the correct physics of how gradually a system absorb energies from applied harmonic potentials (HP) over time to evolve into those states. For that reason, the system’s internal energies are not changed as instantaneously as by a single Heaviside function of time  $t$  [6].

The resulting relationship between Hamiltonian-related work  $W_{\text{total}}$  {or  $W_{\text{H}} = \int_{t_1}^{t_2} [\partial H(\mathbf{z}, \lambda(t)) / \partial t] dt$ } and  $W_{\text{mech}}$  [or  $W_{\text{exp}}$  Eq. (2)] is as clear as the expression given by Eq. (8). As indicated by the identity Eq. (10)  $W_{\text{total}}$  should not appear in Eq. (1). Our theory provides a simple proof that mechanical work  $W_{\text{mech}}$  (or  $W_{\text{exp}}$ ) does appear in JE Eq. (1). If the first term in Eq. (8) has the order of thermal fluctuations ( $\sim k_{\text{B}}T$ ), it is impossible to distinguish  $W_{\text{total}}$  from  $W_{\text{mech}}$  by measurements. This coincidence might have caused the confusion about the definitions of work used in JE. The expression of  $W_{\text{mech}}$  Eq. (9) agrees with the one used for stochastic processes [5, 29, 34] in which JE clearly holds. Therefore, the concerns of time-dependent Hamiltonian [6] or heat baths [7] having influences on the validity of JE might be less severe.

We have shown that it is possible to construct work distributions from the distributions of an RC in both the sequential and parallel pulling simulations (described in Sections III and IV). An acceptable agreement of  $\Delta F^{\text{JE}}(\lambda_s, \lambda_1, k)$  evaluated in the simulations with the PMF profile (Fig. 3) confirms that the sequential and parallel pulling protocols (SPP and PPP) are reasonable. In our protocols, one first has to choose a set of targeted

configurations that can be characterized by different values of  $\lambda$  (the center of an HP). He then independently or sequentially turns on the HP to drive the system into those targeted configurations from any chosen state  $x_0$  (see Section III for details).

In terms of computation expense, the parallel pulling simulations (Section IV Part B) are at least 20 times faster than the sequential ones (Section IV Part A) and have the cost equal to performing 100 trajectories with pulling speed  $v = 10$  Å/ns using the PMF method [13]. In the PMF method, a finite number ( $N_{\text{p}}$ ) of parallel forward-pulling trajectories, as illustrated in Fig. 1a, would produce FEDs that are likely pulling-speed dependence [13, 14, 21, 22]. It has been not clear how to guarantee that the pulling protocol used in the PMF method produces rare states that have a major contribution to work distributions in MD simulations. Kofke *et al.* [35, 36] suggested that the overlapping of the work distributions constructed in forward- and reverse-pulling processes should be adequate to ensure rare small values of work. In other words, one might have to perform more simulations of reverse pulling for examining the accuracy of work distributions constructed in forward pulling simulations. It is possible to carry out such reverse pulling in experiments and use the Crooks fluctuation theorem to examine the distributions of work [3, 9, 10]. Unfortunately, in MD simulations the reverse pulling can be tedious and computationally challenging since the time scales for this reverse pulling can be large for complicated systems [37]. Based on our theory and the simulation results in Section IV, we propose a criterion that overlaps ( $\sim 1.0$  Å) among successive  $x_i$ ’s distributions should be appropriately comparable to their standard deviations, as schematically described in Fig. 1b. If the SPP and PPP meet the criterion, one can carry out only forward-pulling simulations to produce reliable work distributions.

The overlapping requirement of the distributions of the RC resembles the one optimized by solving non-linear equations in the Umbrella Sampling (US) with weighted histogram analysis method [23-25]. The distributions (histograms) in the US method are weighted with restraining potentials to compute probabilities of finding configurations in which a system resides. Then the free energy profile of a pathway is calculated from these probabilities. But work distributions along that pathway cannot be constructed from the histograms of an RC since the expression of work in terms of an RC is not available in the US method.

In addition, we have shown that averaged values of an RC can be used for estimating FEDs based on Eq. (14). In the limit of slow pulling, i.e., infinitely small  $\Delta\lambda$  (large pulling steps  $s$ ), Eq. (14) becomes well-known TI [20, 26] and similar to Adaptive Biasing Force equations [14, 27]:

$$\Delta F_{\text{fluct}}(\lambda_s, \lambda_1, k) \xrightarrow{\Delta\lambda \rightarrow 0} \int_{\lambda_1}^{\lambda_s} \left\langle \frac{\partial H(\lambda, x)}{\partial \lambda} \right\rangle_{\lambda} d\lambda = - \int_{\lambda_1}^{\lambda_s} \langle f_a(x) \rangle_{\lambda} d\lambda, \quad (15)$$



where  $\langle f_a(x) \rangle_\lambda$  are averaged adaptive forces exerted on an RC along a pathway. In the ABF method one has to collect all possible external forces from  $s$  windows in comparison with only  $s-1$  ones as in Eq. (14). Hence, the difference between  $\Delta F_{\text{fluct}}(\lambda_s, \lambda_1, k)$  and  $\Delta F_{\text{ABF}}$  at the same finite increment  $\Delta\lambda$  is  $\Delta\lambda \langle f_s \rangle \approx -\Delta\lambda \langle f_a(x) \rangle_\lambda$ , where  $\langle f_s \rangle$  [see Eq. (9)] is the final averaged force measured at  $\lambda = \lambda_s$ . The error of the ABF method is proportional to square root of  $|\Delta\lambda \langle f_a(x) \rangle_\lambda|$ . Accordingly, at the lowest order of error with a sufficiently large number of available data (large  $s$  and long relaxation time  $\tau$ ), the accuracy of  $\Delta F_{\text{fluct}}(\lambda_s, \lambda_1, k)$  and  $\Delta F_{\text{ABF}}$  is the same. The ABF method does not require specifying any forms of applied forces that are adaptive or constrained along pathways. In our method [Eq. (14)], no constraint is imposed on applied forces. Importantly, the behaviors of the averaged accumulating forces (see the inset in Fig. 3b) in the SPP and PPP are almost the same. Moreover, with appropriate HPs having strong spring constants  $k$  it does not take large  $\tau$  to collect reasonable averaged values of an RC  $\langle x_i \rangle$  along a pathway for free energy calculations (see Fig. 5a). These two important results suggest that FEDs can be evaluated by performing such PPPs to measure  $\langle x_i \rangle$  or averaged accumulating forces along pathways without applying any constraints on external forces.

The introduction of Eq. (14) for evaluating FEDs turns out to be useful to examine the reliability of work distributions used in JE Eq. (12). As shown in Section IV, the accuracy of FEDs computed by Eqs. (12) and (14) depend upon a number of pulling steps  $s$  (related to increment  $\Delta\lambda$ ), relaxation time  $\tau$  and spring constant  $k$ . A strategy to extract the accuracy from our methods is to compare FEDs computed by JE and by Eq. (14). Given finite  $s$  and  $\tau$ , JE usually overestimates FEDs and Eq. (14) underestimates FEDs (see Figs. 3, 4 and 5). It might not be sufficient to just rely on the FEDs computed by either JE or Eq. (14). The FEDs computed by Eq. (12) strongly depend on the quality of rare work distributions and Eq. (14) is an approximation. Equation (14) can be used in the test case for an acceptable accuracy at many values of spring constant  $k$  (see Fig. 4a) and relaxation time  $\tau$  as small as 0.4 ns. But FEDs computed by JE Eq. (12) show strong dependence on  $k$  and  $\tau$  (see Figs. 4b and 5a). Using both the equations, one can estimate how many pulling steps ( $s$  values of  $\lambda$ ) needed to have FEDs equal to  $[\Delta F^{\text{JE}}(\lambda_s, \lambda_1, k) + \Delta F_{\text{fluct}}(\lambda_s, \lambda_1, k)]/2$  with an uncertainty equal to  $[\Delta F^{\text{JE}}(\lambda_s, \lambda_1, k) - \Delta F_{\text{fluct}}(\lambda_s, \lambda_1, k)]/2$ . If the uncertainty is large, one should check the mutual overlapping portions among adjacent distributions of an RC. If those portions are small, it is advisable to reduce the magnitude of spring constants or increase the number of pulling steps (reduce  $\Delta\lambda$ ). If those are too large, it is better to increase the magnitude of spring constants; otherwise the relaxation time should be large.

In conclusion, we suggest that mechanical work  $W_{\text{mech}}$  Eq. (9) should be the work used for JE but in general not  $W_{\text{H}} = \int_{t_1}^{t_2} [\partial H(\mathbf{z}, \lambda(t)) / \partial t] dt$ , even though they become

identical in slow pulling protocols. Our theory differs from previous studies on JE in a way that our work distributions are constructed from the distributions of an RC. The theory suggests a formula [Eq. (14)] that enables us to evaluate FEDs from averaged values of the RC  $\langle x_i \rangle$  along a pathway. We show that it is possible to generate work distributions in sequential and parallel step-wise pulling protocols. In order to use JE Eq. (12) and Eq. (14) with a finite number of pulling steps and reasonably small relaxation time, the quality of the mutual overlapping among adjacent configurations must be taken into account. The combination of JE Eq. (12) and Eq. (14) can be used to estimate FEDs with an uncertainty equal to half of the difference between the FEDs computed by the equations. We show in a test case that our methods require only 19 parallel simulations and relaxation time as small as 0.4 ns for each simulation to estimate FEDs with an uncertainty of about 13%.

## ACKNOWLEDGMENT

We acknowledge Drs. Nakano, Kalia, Nomura and Vemparala for valuable discussions.

## APPENDIX A: SINGLE PULLING STEP

Here we explicitly derive Eqs. (5) and (6) with the assumption that canonical ensembles of  $x_0$  and  $x_1$  exist. Averaging of  $\exp(-\beta W_{\text{H}})$  over  $x_1$ 's ensemble is computed as

$$\begin{aligned} \left\langle e^{-\beta W_{\text{H}}} \right\rangle_{(x_1, \lambda_1, k)} &= \frac{\int d\bar{r}^{3N-1} dx_1 e^{-\beta(W_{\text{H}} + H_0(\bar{r}^{3N-1}, x_1) + \frac{k}{2}(x_1 - \lambda_1)^2)}}{\int d\bar{r}^{3N-1} dx_1 e^{-\beta(H_0(\bar{r}^{3N-1}, x_1) + \frac{k}{2}(x_1 - \lambda_1)^2)}} \\ &= \frac{\int d\bar{r}^{3N-1} dx_1 e^{-\beta \left[ \frac{k}{2}(x_0 - \lambda_1)^2 + H_0(\bar{r}^{3N-1}, x_1) \right]}}{Z(\lambda_1, k)} \\ &= e^{-\beta \frac{k}{2}(x_0 - \lambda_1)^2} \frac{\int d\bar{r}^{3N-1} dx_1 e^{-\beta H_0(\bar{r}^{3N-1}, x_1)}}{Z(\lambda_1, k)} \\ &\Leftrightarrow \left\langle \exp \left\{ -\beta \frac{k}{2} \left[ (x_0 - \lambda_1)^2 - (x_1 - \lambda_1)^2 \right] \right\} \right\rangle_{(x_1, \lambda_1, k)} \\ &= \exp \left[ -\beta \frac{k}{2} (x_0 - \lambda_1)^2 \right] \exp[\beta \Delta F(\lambda_1, k)]. \end{aligned}$$

Since a single value of  $x_0$  at time  $t_0$  is constant in the average, we cancel both sides the factors related to  $x_0$ . Thus, we arrive at Eq. (5):

$$\left\langle \exp \left[ \beta \frac{k}{2} (x_1 - \lambda_1)^2 \right] \right\rangle_{(x_1, \lambda_1, k)} = \exp[\beta \Delta F(\lambda_1, k)].$$

A similar procedure can be carried out to derive Eq. (6):

$$\left\langle e^{-\beta W_{\text{H}}} \right\rangle_{(x_0, k=0)} = \frac{\int d\bar{r}^{3N-1} dx_0 e^{-\beta(W_{\text{H}} + H_0(\bar{r}^{3N-1}, x_0))}}{\int d\bar{r}^{3N-1} dx_0 e^{-\beta H_0(\bar{r}^{3N-1}, x_0)}}$$

$$= e^{\beta \frac{k}{2}(x_1 - \lambda_1)^2} \frac{\int d\vec{r}^{3N-1} dx_0 e^{-\beta \left[ \frac{k}{2}(x_0 - \lambda_1)^2 + H_0(\vec{r}^{3N-1}, x_0) \right]}}{Z(0)}$$

$$\Leftrightarrow \Delta F(\lambda_1, k) = -\beta^{-1} \log \left\langle \exp \left[ -\beta \frac{k}{2}(x_0 - \lambda_1)^2 \right] \right\rangle_{(x_0, k=0)}.$$

## APPENDIX B: SERIES OF PULLING STEPS

The total work absorbed by the system in a series of pulling steps is given by

$$W_{\text{total}} = \int_{t_1}^{t_s} \frac{\partial H(\lambda_1, \lambda_2 \dots \lambda_s, x)}{\partial t} dt = \int_{t_1}^{t_s} \frac{\partial}{\partial t} [H_0(\vec{r}^{3N-1}, x) + \frac{k}{2} \sum_{i=1}^s (x - \lambda_i)^2 \theta(t - t_{i-1}) \theta(t_i - t)] dt$$

$$= \frac{k}{2} [(x_0 - \lambda_1)^2 - (x_s - \lambda_s)^2] + \frac{k}{2} \sum_{i=1}^{s-1} [(\lambda_{i+1} - x_i)^2 - (x_i - \lambda_i)^2]$$

$$= \frac{k}{2} [(x_0 - \lambda_1)^2 - (x_s - \lambda_s)^2] + \sum_{i=1}^{s-1} [H(\lambda_{i+1}, x_i) - H(\lambda_i, x_i)]. \quad (\text{B.1})$$

Since all  $x_i$ 's ensembles are canonical and independent, the average of  $\exp(-\beta W_{\text{total}})$  is computed as

$$\left\langle e^{-\beta W_{\text{total}}} \right\rangle_{(x_0, x_1, \dots, x_s)} = \frac{\int d\vec{r}^{3N-1} dx_0 e^{-\beta H_0(\vec{r}^{3N-1}, x_0)} e^{-\beta \frac{k}{2}(x_0 - \lambda_1)^2}}{Z(0)}$$

$$\times \frac{\prod_{i=1}^{s-1} \int d\vec{r}^{3N-1} dx_i e^{-\beta (H_0(\vec{r}^{3N-1}, x_i) + \frac{k}{2}(x_i - \lambda_i)^2)} e^{-\beta \frac{k}{2}(x_i - \lambda_{i+1})^2 - (x_i - \lambda_i)^2}}{Z(\lambda_1, k) \dots Z(\lambda_{s-1}, k)}$$

$$\times \frac{\int d\vec{r}^{3N-1} dx_s e^{-\beta (H_0(\vec{r}^{3N-1}, x_s) + \frac{k}{2}(x_s - \lambda_s)^2)} e^{-\beta \frac{k}{2}(x_s - \lambda_s)^2}}{Z(\lambda_s, k)} = 1. \quad (\text{B.2})$$

By definition  $W_{\text{mech}}$  does not contain  $x_0$  and  $x_s$ , we first take the average of  $\exp(-\beta W_{\text{total}})$  over these variables:

$$\left\langle e^{-\beta W_{\text{total}}} \right\rangle_{x_0, x_s} = \frac{\int d\vec{r}^{3N-1} dx_0 e^{-\beta (H_0(\vec{r}^{3N-1}, x_0) + \frac{k}{2}(x_0 - \lambda_1)^2)}}{Z(0)} \times \frac{\int d\vec{r}^{3N-1} dx_s e^{-\beta H_0(\vec{r}^{3N-1}, x_0)} e^{-\beta W_{\text{mech}}}}{Z(\lambda_s, k)}$$

$$= e^{\beta [F(\lambda_s, k) - F(\lambda_1, k)]} e^{-\beta W_{\text{mech}}}. \quad (\text{B.3})$$

It is noted that all possible values of  $W_{\text{mech}}$  can be constructed from either force-versus-extension (FVE) curves or from the ensembles of  $x_i$  with  $i$  from 1 to  $s-1$  based on Eq. (9). Therefore, averaging the left hand side of Eq. (B3) over all possible FVE curves is equal to averaging the right hand side over the rest of  $x_i$ . Taking this observation into account and using the identity (B.2), we arrive at a formula identical to JE:

$$\Delta F^{\text{JE}}(\lambda_s, \lambda_1, k) = -\beta \ln \left\langle e^{-\beta W_{\text{mech}}} \right\rangle_{\text{FVE}}. \quad (\text{B.4})$$

Furthermore,  $x_i$ 's distributions can be approximated as  $\exp[-\beta k(x_i - \langle x_i \rangle)^2 / (2\gamma_i^2)]$ , where  $\langle x_i \rangle$  is the averaged position of the RC at  $i^{\text{th}}$  pulling step and  $\gamma_i^2$  is equal to  $k\sigma_i^2/k_{\text{B}}T$  with  $\sigma_i$  equal to the standard deviation of  $x_i$ 's distribution. If all increments  $\lambda_{i+1} - \lambda_i$  are the same as  $\Delta\lambda = (\lambda_s - \lambda_1)/s$ , we derive an analytical expression for the left hand side of Eq. (B.4):

$$\left\langle \exp[-\beta W_{\text{mech}}] \right\rangle_{\text{FVE}} = \frac{\int dW_{\text{mech}} \rho(W_{\text{mech}}) e^{-\beta W_{\text{mech}}}}{\int dW_{\text{mech}} \rho(W_{\text{mech}})} \quad (\text{B.5})$$

$$\equiv \prod_{i=1}^{s-1} \frac{\int dx_i \exp \left\{ -\beta k \left[ \frac{(x_i - \langle x_i \rangle)^2}{2\gamma_i^2} + \frac{\Delta\lambda(2\lambda_i + \Delta\lambda - 2x_i)}{2} \right] \right\}}{\int dx_i \exp[-\beta k (x_i - \langle x_i \rangle)^2 / 2\gamma_i^2]}$$

$$= \prod_{i=1}^{s-1} \exp \left\{ -\frac{\beta k \Delta\lambda^2}{2} [(1 - \gamma_i^2) + 2 \frac{\lambda_i - \langle x_i \rangle}{\Delta\lambda}] \right\}.$$

$$\Rightarrow \Delta F^{\text{G}}(\lambda_s, \lambda_1, k) = \frac{k\Delta\lambda^2}{2} \sum_{i=1}^{s-1} (1 - \gamma_i^2) + k\Delta\lambda \sum_{i=1}^{s-1} (\lambda_i - \langle x_i \rangle).$$

## APPENDIX C: WORK DISTRIBUTION CONSTRUCTION

Given  $\lambda_1$ ,  $\lambda_s$ ,  $\Delta\lambda$  and a data set of  $x_i$  we divide a sufficiently large interval into  $K$  bins with a width of  $\delta x$ . This interval can contain all values of  $x_i$ . For example, we choose the interval to be 50.0 Å with  $\delta x = 0.001$  Å. The distributions of  $x_i$   $\rho_i(x_i)$  are constructed by counting probability of  $x_i$  falling into each bin. Similarly, we estimate a range that all mechanical work  $W_{\text{mech}}$  ( $W_1, W_2 \dots W_{s-1}$ ) can fall into, for instance, 200.0 kcal/mol with a bin width  $\delta W = 0.01$  kcal/mol.  $M$  (20,000) bins are available for  $W_{\text{mech}}$ . As pulling step  $i$  is equal to 1,  $W_1$  is zero [see Eq. (9)]. As pulling step  $i$  is equal to 2, we construct the distribution of  $W_2$ , here denoted by  $\Omega_2(W_2)$ , as in the following pseudo-code:

```
for (j = 1; j ≤ K; j++) {
  if (ρ1(j) ≠ 0) { // ρ1(x1) are non-zero in small
    regions around x1.
    W2 = kΔλ(2λ1 - 2jδx + Δλ)/2;
    w = INT(W2/δW); // transform a real number
    into an integer.
    Ω2(w) = ρ1(j); // all Ωi>2 are initialized to
    be zero.
  }
}
```

As pulling steps  $i$  are greater than 2, the work distributions of these pulling steps are accumulated as the following:

```
for (i = 3; i ≤ s - 1; i++) { // i should not exceed
  s - 1 because we don't want to compute FED at λ = λs
  + Δλ.
  for (j = 1; j ≤ K; j++) {
    if (ρi-1(j) ≠ 0) {
      for (w1 = -M; w1 ≤ M; w1++) {
        if (Ωi-1(w1) ≠ 0) {
```

$$W_i = w_1 \times \delta W + k\Delta\lambda(2\lambda_{i-1} - 2j\delta x + \Delta\lambda)/2;$$

$$w_2 = \text{INT}(W_i/\delta W);$$

$$\Omega_i(w_2) += \rho_{i-1}(j) \times \Omega_{i-1}(w_1);$$

}}}}}

We observe that INT function produces an unwanted spike appearing in work distributions at  $W_i = 0.0$ . We smooth work distributions at this value by assigning  $\Omega_i(0) = [\Omega_i(-1) + \Omega_i(1)]/2$ . From the distributions of work  $\Omega_i$ , it is straightforward to compute FEDs based on Eq. (12) or Eq. (B.5). The error analysis of these numerical calculations can be found elsewhere [14, 38]. The variance of FEDs can be estimated by  $\frac{\sigma_W^2}{Q} + \frac{\beta^2 \sigma_W^4}{2(Q-1)}$ , where  $\sigma_W$  are the standard deviations of work distributions  $\Omega_i(W_i)$  and  $Q$  is a number of bins which have non-zero  $\Omega_i(W_i)$ . For example, at the sequential pulling step  $i = 35$  (see Fig. 2b)  $\sigma_W$  of the corresponding work distribution is about 10 kcal/mol with  $Q \sim 20000$ , then the variance is about 0.7 kcal/mol at temperature  $T = 300$  K. Thus the standard deviation of the corresponding FED is about 0.8 kcal/mol. This deviation is about two times smaller than half of the difference ( $\sim 2.0$  kcal/mol) between  $\Delta F^{\text{JE}}(\lambda_s, \lambda_1, k)$  and  $\Delta F_{\text{fluct}}(\lambda_s, \lambda_1, k)$  in Section IV Parts B and D. Larger  $Q$  (larger  $K$  and  $M$ ) is observed to not make the difference smaller, even though it reduces the deviation. Therefore, we choose  $[\Delta F^{\text{JE}}(\lambda_s, \lambda_1, k) - \Delta F_{\text{fluct}}(\lambda_s, \lambda_1, k)]/2$  as the major uncertainty of our methods. We find that the choices of  $\delta x$  and  $\delta W$  give reasonable estimates of work distributions and their FEDs in all cases of investigated spring constants and relaxation time.

---

[1] C. Jarzynski, Physical Review Letters **78**, 2690 (1997).  
[2] J. T. Liphardt *et al.*, Biophysical Journal **82**, 193A (2002).  
[3] D. Collin *et al.*, Nature **437**, 231 (2005).  
[4] F. Douarche, and et al., EPL (Europhysics Letters) **70**, 593 (2005).  
[5] C. Jarzynskia, The European Physical Journal B - Condensed Matter and Complex Systems **64**, 331 (2008).  
[6] J. M. G. Vilar, and J. M. Rubi, Physical Review Letters **100** (2008).  
[7] E. G. D. Cohen, and D. Mauzerall, Journal of Statistical Mechanics-Theory and Experiment (2004).  
[8] C. Jarzynski, Comptes Rendus Physique **8**, 495.  
[9] G. E. Crooks, Physical Review E **60**, 2721 (1999).  
[10] G. E. Crooks, Physical Review E **61**, 2361 (2000).  
[11] L. Y. Chen, Journal of Chemical Physics **129** (2008).  
[12] G. E. Crooks, The Journal of Chemical Physics **130**, 107101 (2009).

[13] S. Park *et al.*, Journal of Chemical Physics **119**, 3559 (2003).  
[14] D. Rodriguez-Gomez, E. Darve, and A. Pohorille, Journal of Chemical Physics **120**, 3563 (2004).  
[15] H. Oberhofer, C. Dellago, and P. L. Geissler, Journal of Physical Chemistry B **109**, 6902 (2005).  
[16] D. A. Hendrix, and C. Jarzynski, The Journal of Chemical Physics **114**, 5974 (2001).  
[17] D. K. West, P. D. Olmsted, and E. Paci, The Journal of Chemical Physics **125**, 204910 (2006).  
[18] S. Park, and K. Schulten, The Journal of Chemical Physics **120**, 5946 (2004).  
[19] B. Isralewitz, M. Gao, and K. Schulten, Current Opinion in Structural Biology **11**, 224 (2001).  
[20] G. Hummer, Journal of Chemical Physics **114**, 7330 (2001).  
[21] T. Bastug *et al.*, The Journal of Chemical Physics **128**, 155104 (2008).  
[22] T. Bastug, and S. Kuyucak, Chemical Physics Letters **436**, 383 (2007).  
[23] G. M. Torrie, and J. P. Valleau, Journal of Computational Physics **23**, 187 (1977).  
[24] S. Kumar *et al.*, Journal of Computational Chemistry **13**, 1011 (1992).  
[25] M. Souaille, and B. Roux, Computer Physics Communications **135**, 40 (2001).  
[26] P. Kollman, Chemical Reviews **93**, 2395 (1993).  
[27] E. Darve, and A. Pohorille, Journal of Chemical Physics **115**, 9169 (2001).  
[28] R. W. Zwanzig, The Journal of Chemical Physics **22**, 1420 (1954).  
[29] G. Crooks, Journal of Statistical Physics **90**, 1481 (1998).  
[30] G. Schay, *Introduction to Probability with Statistical Applications* (Birkhauser Boston, Boston, 2007), p. 313.  
[31] M. P. Allen, and D. J. Tildesley, *Computer Simulation of Liquids* (Oxford University Press, 2003), p. 213.  
[32] L. Kale *et al.*, Journal of Computational Physics **151**, 283 (1999).  
[33] A. D. MacKerell *et al.*, Journal of Physical Chemistry B **102**, 3586 (1998).  
[34] C. Jarzynski, Physical Review E **56**, 5018 (1997).  
[35] D. A. Kofke, Molecular Physics **104**, 3701 (2006).  
[36] N. D. Lu, D. A. Kofke, and T. B. Woolf, Journal of Computational Chemistry **25**, 28 (2004).  
[37] Y. Duan, and P. A. Kollman, Science **282**, 740 (1998).  
[38] D. M. Zuckerman, and T. B. Woolf, Physical Review Letters **89** (2002).